

1 **Japanese mayfly family classification with a vision transformer model**

2

3 Yuichi Iwasaki^{1,5,*}, Hiroko Arai^{2,6,9*}, Akihiro Tamada^{3,7}, Hirokatsu Kataoka^{4,8}

4 ¹ National Institute of Advanced Industrial Science and Technology (AIST), Research Institute of
5 Science for Safety and Sustainability, 16-1 Onogawa, Tsukuba, Ibaraki 305-8569, Japan

6 ² National Institute of Advanced Industrial Science and Technology (AIST), Research Center for
7 Emerging Computing Technologies, 1-1-1 Umezono, Tsukuba, Ibaraki 305-8568, Japan

8 ³ Graduate School of Life Sciences, Tohoku University, Miyagi 980-0812, Japan

9 ⁴ National Institute of Advanced Industrial Science and Technology (AIST), Artificial Intelligence
10 Research Center (AIRC), 1-1-1 Umezono, Tsukuba, Ibaraki 305-8560, Japan

11

12 Corresponding authors: Hiroko Arai (arai-h@aist.go.jp) and Yuichi Iwasaki (yuichiwsk@gmail.com,
13 yuichi-iwasaki@aist.go.jp)

14 *These authors equally contributed to this work

15

16 Total number of words (text body): 2443

17 Total number of figures: 5

18 Total number of tables: 2

19 **Abstract**

20 Benthic macroinvertebrates are a frequently used indicator group for biomonitoring and biological
21 assessment of river ecosystems. However, their taxonomic identification is laborious and requires
22 special expertise. In this study, we aimed to assess the capability of a vision transformer (ViT) model for
23 family-level identification of mayflies (order Ephemeroptera). Specifically, we focused on evaluating
24 the model's capacity to classify three commonly found mayfly families (Baetidae, Ephemerellidae, and
25 Heptageniidae) as well as other families that were grouped together. For the modeling, we originally
26 constructed two different image datasets containing a total of 1,110 images of mayflies, which were split
27 into training and validation datasets, and a test dataset was prepared from two different online photo
28 galleries. The developed ViT model achieved reasonable accuracy, reaching 94.2% and 82.9% for the
29 validation and test datasets, respectively. Given the use of a relatively small number of images in the
30 training process, as well as some variations in the visual styles of the test dataset compared to the training
31 dataset, we consider the level of accuracy to be high. Our results are encouraging toward the use of
32 computer vision for taxonomic identification of macroinvertebrates, although there is still a need to
33 develop specific designs and plans for this purpose, which can vary depending on regional differences
34 in biodiversity as well as sampling and survey methods.

35 **Keywords**

36 Macroinvertebrate; Aquatic insect; Machine learning; Pattern recognition; Computer vision

37

38 **Introduction**

39 Freshwater covers less than 1% of the Earth's surface (Garcia-Moreno et al. 2014) and accounts for only
40 2.5% of the Earth's water resources (Garcia-Moreno et al. 2014; Oki &Kanae 2006). Despite their
41 relatively small size, freshwater ecosystems support approximately 10% of all known species (Román-
42 Palacios et al. 2022) and provide vital material, non-material, and regulating services for humans (Lynch
43 et al. 2023). However, the marked degradation of freshwater ecosystems and loss of freshwater
44 biodiversity highlight the importance of their conservation (Loh et al. 2005; Poff et al. 2007; Reid et al.
45 2019; Tickner et al. 2020). To assess the biological/ecological status of freshwaters such as streams and
46 rivers, biomonitoring using algae, macroinvertebrates, fish, and other species is essential. Among these
47 groups, river benthic macroinvertebrates are most frequently used as a bioindicator group worldwide
48 (Birk et al. 2012; Buss et al. 2015; Eriksen et al. 2021; Namba et al. 2020).

49 Benthic macroinvertebrates have many characteristics that make them useful for biomonitoring,
50 such as their relatively sedentary nature, ease of sampling, and diverse sensitivities to stressors (Buss et
51 al. 2015; Eriksen et al. 2021; Rosenberg et al. 2008), but sorting and taxonomic identification of benthic
52 macroinvertebrate samples are laborious tasks that require the expertise of specialists (Ärje et al. 2020b).
53 Particularly when a single family can be represented by multiple genera and species, species or genus-
54 level identifications usually require the examination of morphological characteristics under a

55 microscope because they are unlikely to be visible in whole-body photographs of individuals. In contrast,
56 family-level identification can often be accomplished with the naked eye. The level of identification
57 required for environmental assessments has been a topic of discussion (Buss et al. 2015; Jones 2008),
58 but many macroinvertebrate indices based on family-level identifications, such as the Biological
59 Monitoring Working Party (BMWP) system (Armitage et al. 1983), are used globally (Buss et al. 2015).
60 Therefore, particularly in cases where a single family comprises multiple genera and species,
61 endeavoring family-level identification through image recognition represents a feasible and pragmatic
62 goal.

63 Image recognition is one of the most successful advancements in machine learning technology.
64 Thanks to the development of convolution neural networks (CNNs) and their derivative techniques, the
65 recognition performance of computer vision is now as good as human recognition in some cases (He et
66 al. 2016; Russakovsky et al. 2015). Although transformers were originally developed for natural
67 language processing, the vision transformer (ViT) has emerged as a useful technique for image
68 recognition in the field of computer vision. The recognition performance of ViT-based models
69 outperforms that of CNN-based models in some aspects (Dosovitskiy et al. 2021). However, to our
70 knowledge, the use of ViT-based models for the species identification of river macroinvertebrates has
71 not been explored.

72 While several previous studies have implemented automated species identification for river

73 benthic macroinvertebrates using machine learning techniques through image recognition (Ärje et al.
74 2020b; Joutsijoki et al. 2014; Larios et al. 2011; Lytle et al. 2010; Milosavljević et al. 2021; Raitoharju
75 et al. 2018), many of these studies used datasets with a limited number of species within a single family
76 (but see Larios et al. 2011; Milosavljević et al. 2021). In this study, our objective was to assess the
77 capability of a ViT model for family-level identification of mayflies (order Ephemeroptera), considering
78 the presence of multiple taxa (i.e., genus/species) within a single family. Specifically, our focus was to
79 evaluate the capacity for classifying the three mayfly families (Baetidae, Ephemerellidae, and
80 Heptageniidae) found commonly in Japanese rivers, as well as another group that contained several other
81 families within the order Ephemeroptera. These three families have varied sensitivities to organic and
82 metal pollution. For example, ephemerellid and heptageniid mayflies are highly responsive to metal and
83 organic pollution in the environment, whereas baetid mayflies are often found in metal- and organic-
84 contaminated rivers (Armitage et al. 1983; Iwasaki et al. 2018a; Iwasaki et al. 2018b). Recently, an
85 attempt was made to assess the levels of ecological impacts in metal-contaminated rivers mainly on the
86 basis of changes in the abundances or presence/absence of these three families (Iwasaki et al. 2023),
87 indicating their importance as indicators for environmental impact assessments.

88

89 **Materials and Methods**

90 *Dataset construction*

91 The image datasets used in this study were originally created by two individuals—A. Tamada (T-dataset)
92 and M. Monma (M-dataset)—who independently collected and identified mayflies, along with other
93 insects, from rivers in Japan for their own personal interests. Although the mayflies were identified
94 generally to genus or species level, we used the family-level results in this study. The images of mayflies
95 were captured either directly with a digital camera or using a digital camera attached to stereo
96 microscope, manually labeled, and saved in JPG format. Both datasets consisted of close-up photos of
97 insects captured mostly from an overhead perspective, either against a black background (T-dataset, Fig.
98 1a) or with a ruler in the background (M-dataset, Fig. 1b). Both datasets contained images of 8 aquatic
99 insect families in the order Ephemeroptera: Baetidae, Ephemerellidae, Heptageniidae, Ameletidae,
100 Ephemeridae, Leptophlebiidae, Oligoneuriidae, and Siphonuridae. Because both datasets had more
101 images of the former three families than of the latter four families, the latter families were combined
102 into one class (D, other mayflies; Table 1). The T- and M-datasets included 5 and 12 taxa (unique species
103 or genus) in Baetidae, 17 and 13 taxa in Ephemerellidae, and 13 and 14 taxa in Heptageniidae,
104 respectively.

105 The images were randomly divided: 80% into a training dataset and 20% into a validation
106 dataset for each class in each dataset. The respective training and validation datasets were then combined
107 (Table 1). The total number of images in the training dataset (N_{train}) was 885, and the total in the
108 validation dataset (N_{val}) was 225. To examine the potential impact of dataset composition, five train/val

109 datasets with different configurations were prepared by randomly selecting images for training and
110 validation splits.

111 We also prepared a test dataset consisting of images collected from two different online photo
112 galleries (Table 2). The styles of the images in these galleries differed from those of the images used for
113 training; for instance, the background was white/gray or blue. As above, the “other mayflies” group
114 included five families (Ameletidae, Ephemeridae, Leptophlebiidae, Oligoneuriidae, and Siphonuridae).

115

116 *Mayfly classification model*

117 To develop a recognition model for classifying mayfly families, we adopted the fine-tuning technique,
118 which additionally trains the “classifier” of the pre-trained model and is an effective way to build a
119 recognition model of a specific dataset that is difficult to scale up (Brigato et al. 2022). A schematic
120 illustration of the three steps used to construct the mayfly classification model is shown in Fig. 2. Here,
121 we used the pre-trained ViT model provided by Kataoka et al. (2022), which was constructed in two
122 steps (Fig. 2). In the first step, a model was trained from scratch with a fractal database created by using
123 mathematical information of fractal images. In the second step, the model was fine-tuned with ImageNet,
124 which is a large-scale real image dataset. In these steps, the model gains the ability to recognize real
125 images. In the third step, the pre-trained ViT model was further fine-tuned with our mayfly dataset. The
126 latter fine-tuning step was performed using the training codes provided by Kataoka et al. (2022)

127 (available at <https://github.com/masora1030/CVPR2022-Pretrained-ViT-PyTorch>), with the default
128 settings, except for the number of classes and the method used to calculate accuracy. The training code
129 was modified to calculate the “top-1” accuracy of 4-class classification task. The top-1 accuracy was
130 calculated as the ratio of the number of images predicted correctly by the class with the highest
131 confidence score to the total number of validation images (N_{val}). Similar to CNN-based image
132 recognition, ViT-based models output a confidence score for each class. This score indicates the
133 probability that the image belongs to a particular class. The class with the highest confidence score was
134 assigned as the predicted class. In the default settings of the training code, the images input into the pre-
135 trained model are resized to $224 \times 224 \times 3$ RGB images. During training, additional data argumentation
136 methods were applied to the resized images. They were randomly cropped after they had been randomly
137 converted with different aspect ratios, and then the brightness, contrast, and saturation of color (i.e.,
138 color jitter) were also randomly changed. During validation, the resized images were directly input to
139 the model without data argumentation. The recognition task with the test dataset was performed by using
140 the timm library (Wightman 2019).

141

142 **Results and Discussion**

143 *Mayfly classification model*

144 Results obtained from one of the five randomly prepared train/val datasets are shown in Fig. 3; similar

145 results were obtained from the other datasets (accuracy: 91.7–94.3%). The learning curves of loss
146 function for training and validation converged to a low value (Fig. 3a), indicating that the fine tuning
147 was successful. The confusion matrix (Fig. 3b) shows the number of images predicted for individual
148 classes. For example, in class A, 54 images were placed correctly, and 1 was placed incorrectly in each
149 class C and class D. The top-1 accuracy was 94.2%. The confidence score and the predicted class of all
150 images in the validation dataset are summarized in Fig. 3c. In classes with true labels A (Baetidae) and
151 C (Heptageniidae), 83% and 87% of the images, respectively, had confidence scores above 80%, and
152 they all were classified correctly. In the case of true label B (Ephemerellidae), 77% of the images had
153 confidence scores above 80%, but a few images with high confidence scores (>80%) were misclassified.
154 In the case of true label D (other mayflies), only 54% of the images had high confidence scores. Of all
155 the misclassified images, 69% had confidence scores below 70%.

156 Example images of classes A, B, and C in the validation dataset are shown in Fig. 4. The
157 distinctions between correctly classified and misclassified images were not readily apparent. Some
158 misclassified images notably lacked the head portion of the mayflies (IDs 73, 91, 134, and 141) due to
159 the resizing of the original images in the default setting of the training code. In all cases, the original
160 image in the dataset included the entire body of the mayflies, and these resized images were also used
161 for fine-tuning. Despite using a relatively small number of images in the training process and employing
162 the default setting (i.e., both the fine-tuning and validation were performed with the resized images,

163 including ones missing body parts), a high recognition rate was attained. This is likely an advantage of
164 using a well pre-trained ViT model on a large natural image dataset such as ImageNet.

165 To evaluate the recognition performance on entirely new images that the model had not been
166 exposed to during training, we used the test dataset, and the results of the classification are shown in Fig.
167 5. Despite some variations in the visual styles between the test and training datasets, the classification
168 accuracy remained high (82.9%). The overall decrease in accuracy was attributed to that in classifying
169 class D because the accuracies for classes A–C were almost identical to those achieved on the validation
170 dataset. Thus, we conclude that the model we built can provide a reasonable level of accuracy for
171 classifying three common mayfly families.

172

173 *Future Directions*

174 This is the first study to develop a ViT model for the identification of Japanese mayfly families. Despite
175 the reasonable level of model accuracy attained, there are issues that need to be addressed for practical
176 implementation. First, to assess biological conditions on the basis of family-level macroinvertebrate
177 identification (Paisley et al. 2014; Torii et al. 2023; Wright 2000) using the ViT model, it is necessary to
178 include other families within mayflies (Ephemeroptera), as well as other orders (e.g., Plecoptera,
179 Trichoptera, and Diptera), which are commonly found in river macroinvertebrate surveys. Second,
180 although biological assessments based on the family-level identification of macroinvertebrates can

181 provide the appropriate amount of information for a given purpose (Jones 2008; Wright & Ryan 2016),
182 more detailed assessments may require identifications to the genus and species levels. As previously
183 noted (Joutsijoki et al. 2014; Raitoharju et al. 2018), a critical barrier to address these two issues is the
184 lack of appropriate images for model development. To this end, the original images used in this study
185 have been made available (see the GitHub website at
186 https://github.com/yuichiwsk/images_mayfly_families). Species- and genus-level identifications also
187 require checking smaller and more detailed morphological characteristics (see, e.g., Merrit et al. 2019),
188 many of which are not visible in the overhead-perspective images used in this study. Thus, such
189 identifications using computer vision and acquiring relevant images become even more challenging.
190 Finally, since the mayfly images used in this study were manually captured from fixed directions, the
191 implementation of semi- or fully-automated imaging and identification poses a further challenge for
192 integrating computer vision into biological assessments based on macroinvertebrates (but see Ärje et al.
193 2020a; Jaballah et al. 2023; Raitoharju et al. 2018). Developing specific designs and plans about how to
194 use computer vision in macroinvertebrate identification, which may vary depending on diverse regional
195 differences in inherent biodiversity as well as sampling and survey methods, is a fundamental challenge
196 that needs to be addressed in future studies.

197

198 **Data availability**

199 All the original image data used for developing the vision transformer model (i.e., training and validation
200 datasets) are available on the GitHub website (https://github.com/yuichiwsk/images_mayfly_families).

201

202 **Acknowledgements**

203 We are deeply grateful to K. Monma for providing the mayfly images. During the preparation of this
204 study, the authors used ChatGPT to improve readability and language. After using this tool, the authors
205 reviewed and edited the content as needed and take full responsibility for the content of the publication.

206

207 **Funding**

208 This research did not receive any specific grant from funding agencies in the public, commercial, or
209 not-for-profit sectors.

210

211 **Author contributions**

212 Yuichi Iwasaki: Conceptualization, Investigation, Data Curation, Writing - Original Draft, Writing -
213 Review & Editing. Hiroko Arai: Conceptualization, Methodology, Software, Formal analysis, Resources,
214 Data Curation, Writing - Original Draft, Writing - Review & Editing, Visualization. Akihiro Tamada:
215 Investigation, Data Curation, Writing - Review & Editing. Hirokatsu Kataoka: Software, Writing -
216 Review & Editing, Supervision.

217

218 **References**

- 219 Ärje J, Melvad C, Jeppesen MR, Madsen SA, Raitoharju J, Rasmussen MS, Iosifidis A, Tirronen V,
220 Gabbouj M, Meissner K, Høye TT (2020a) Automatic image-based identification and biomass
221 estimation of invertebrates. *Methods in Ecology and Evolution* 11:922–931. doi:10.1111/2041-
222 210X.13428
- 223 Ärje J, Raitoharju J, Iosifidis A, Tirronen V, Meissner K, Gabbouj M, Kiranyaz S, Kärkkäinen S (2020b)
224 Human experts vs. machines in taxa recognition. *Signal Process Image Commun* 87:115917. doi:
225 10.1016/j.image.2020.115917
- 226 Armitage PD, Moss D, Wright JF, Furse MT (1983) The performance of a new biological water-quality
227 score system based on macroinvertebrates over a wide-range of unpolluted running-water sites. *Water*
228 *Res* 17:333–347. doi:10.1016/0043-1354(83)90188-4
- 229 Birk S, Bonne W, Borja A, Brucet S, Courrat A, Poikane S, Solimini A, van de Bund WV, Zampoukas
230 N, Hering D (2012) Three hundred ways to assess Europe's surface waters: An almost complete overview
231 of biological methods to implement the Water Framework Directive. *Ecological Indicators* 18:31–41.
232 doi:10.1016/j.ecolind.2011.10.009
- 233 Brigato L, Barz B, L. I, J. D (2022) Image classification with small datasets: overview and benchmark.
234 *IEEE Access* 10:49233–49250. doi:10.1109/ACCESS.2022.3172939

235 Buss DF, Carlisle DM, Chon T-S, Culp J, Harding JS, Keizer-Vlek HE, Robinson WA, Strachan S,
236 Thirion C, Hughes RM (2015) Stream biomonitoring using macroinvertebrates around the globe: a
237 comparison of large-scale programs. *Environmental Monitoring and Assessment* 187:4132.
238 doi:10.1007/s10661-014-4132-8

239 Dosovitskiy A, Beyer L, Kolesnikov A, Weissenborn D, Zhai X, Unterthiner T, Dehghani M, Minderer
240 M, Heigold G, Gelly S, Uszkoreit J, Houlsby N (2021): An image is worth 16x16 words: Transformers
241 for image recognition at scale, *International Conference on Learning Representations*.
242 <https://openreview.net/forum?id=YicbFdNTTy>

243 Eriksen TE, Brittain JE, Søli G, Jacobsen D, Goethals P, Friberg N (2021) A global perspective on the
244 application of riverine macroinvertebrates as biological indicators in Africa, South-Central America,
245 Mexico and Southern Asia. *Ecological Indicators* 126:107609. doi: 10.1016/j.ecolind.2021.107609

246 Garcia-Moreno J, Harrison IJ, Dudgeon D, Clausnitzer V, Darwall W, Farrell T, Savy C, Tockner K,
247 Tubbs N (2014): Sustaining Freshwater Biodiversity in the Anthropocene. In: Bhaduri A, Bogardi J,
248 Leentvaar J, Marx S (Editors), *The Global Water System in the Anthropocene: Challenges for Science*
249 *and Governance*. Springer International Publishing, Cham, Switzerland, pp. 247–270

250 He K, Zhang X, Ren S, Sun J (2016): Deep residual learning for image recognition, *Proceedings of the*
251 *IEEE Conference on Computer Vision and Pattern Recognition (CVPR)*, pp. 770–778

252 Iwasaki Y, Kagaya T, Matsuda H (2018a) Comparing macroinvertebrate assemblages at organic-

253 contaminated river sites with different zinc concentrations: Metal-sensitive taxa may already be absent.
254 Environ Pollut 241:272–278. doi:10.1016/j.envpol.2018.05.041

255 Iwasaki Y, Schmidt TS, Clements WH (2018b) Quantifying differences in responses of aquatic insects
256 to trace metal exposure in field studies and short-term stream mesocosm experiments. Environ Sci
257 Technol 52:4378–4384. doi:10.1021/acs.est.7b06628

258 Iwasaki Y, Mano H, Shinohara N (2023) Linking levels of trace-metal concentrations and ambient
259 toxicity to cladocerans to levels of effects on macroinvertebrate communities. Environ Adv 11:100348.
260 doi:10.1016/j.envadv.2023.100348

261 Jaballah S, Garcia GF, Martignac F, Parisey N, Jumel S, Roussel J-M, Dézerald O (2023) A deep learning
262 approach to detect and identify live freshwater macroinvertebrates. Aquatic Ecology 57:933–949.
263 doi:10.1007/s10452-023-10053-7

264 Jones FC (2008) Taxonomic sufficiency: The influence of taxonomic resolution on freshwater
265 bioassessments using benthic macroinvertebrates. Environ Rev 16:45–69. doi:10.1139/A07-010

266 Joutsijoki H, Meissner K, Gabbouj M, Kiranyaz S, Raitoharju J, Ärje J, Kärkkäinen S, Tirronen V,
267 Turpeinen T, Juhola M (2014) Evaluating the performance of artificial neural networks for the
268 classification of freshwater benthic macroinvertebrates. Ecol Inform 20:1–12.
269 doi:10.1016/j.ecoinf.2014.01.004

270 Kataoka H, Hayamizu R, Yamada R, Nakashima K, Takashima S, Zhang X, Martinez-Noriega EJ, Inoue

271 N, Yokota R (2022): Replacing labeled real-image datasets with auto-generated contours, Proceedings
272 of the IEEE/CVF Conference on Computer Vision and Pattern Recognition, pp. 21232–21241

273 Larios N, Lin J, Zhang M, Lytle D, Moldenke A, Shapiro L, Dietterich T (2011): Stacked spatial-pyramid
274 kernel: An object-class recognition method to combine scores from random trees, 2011 IEEE Workshop
275 on Applications of Computer Vision (WACV), pp. 329–335

276 Loh J, Green RE, Ricketts T, Lamoreux J, Jenkins M, Kapos V, Randers J (2005) The Living Planet
277 Index: using species population time series to track trends in biodiversity. *Philos Trans R Soc B* 360:289–
278 295. doi:10.1098/rstb.2004.1584

279 Lynch AJ et al. (2023) People need freshwater biodiversity. *WIREs Water*:e1633.
280 doi:10.1002/wat2.1633

281 Lytle DA, Martínez-Muñoz G, Zhang W, Larios N, Shapiro L, Paasch R, Moldenke A, Mortensen EN,
282 Todorovic S, Dietterich TG (2010) Automated processing and identification of benthic invertebrate
283 samples. *J N Am Benthol Soc* 29:867–874. doi:10.1899/09-080.1

284 Merritt RW, Cummins KW, Berg MB (2019): An introduction to the aquatic insects of North America.
285 Kendall Hunt Publishing, Dubque, Iowa, 1480 pp

286 Milosavljević A, Milošević Đ, Predić B (2021) Species identification for aquatic biomonitoring using
287 deep residual cnn and transfer learning. *Facta Universitatis, Series: Automatic Control and Robotics*.
288 doi:2010.22190/FUACR201118001M

289 Namba H, Iwasaki Y, Heino J, Matsuda H (2020) What to survey? A systematic review of the choice of
290 biological groups in assessing ecological impacts of metals in running waters. *Environ Toxicol Chem*
291 39:1964–1972. doi:10.1002/etc.4810

292 Oki T, Kanae S (2006) Global hydrological cycles and world water resources. *Science* 313:1068–1072.
293 doi:10.1126/science.1128845

294 Paisley MF, Trigg DJ, Walley WJ (2014) Revision of the biological monitoring working party (BMWP)
295 score system: Derivation of present-only and abundance-related scores from field data. *River Res Appl*
296 30:887–904. doi:10.1002/rra.2686

297 Poff NL, Olden JD, Merritt DM, Pepin DM (2007) Homogenization of regional river dynamics by dams
298 and global biodiversity implications. *Proc Nat Acad Sci USA* 104:5732–5737.
299 doi:10.1073/pnas.0609812104

300 Raitoharju J, Riabchenko E, Ahmad I, Iosifidis A, Gabbouj M, Kiranyaz S, Tirronen V, Ärje J,
301 Kärkkäinen S, Meissner K (2018) Benchmark database for fine-grained image classification of benthic
302 macroinvertebrates. *Image Vis Comput* 78:73–83. doi:10.1016/j.imavis.2018.06.005

303 Reid AJ, Carlson AK, Creed IF, Eliason EJ, Gell PA, Johnson PTJ, Kidd KA, MacCormack TJ, Olden
304 JD, Ormerod SJ, Smol JP, Taylor WW, Tockner K, Vermaire JC, Dudgeon D, Cooke SJ (2019) Emerging
305 threats and persistent conservation challenges for freshwater biodiversity. *Biological Reviews* 94:849–
306 873. doi:10.1111/brv.12480

307 Román-Palacios C, Moraga-López D, Wiens JJ (2022) The origins of global biodiversity on land, sea
308 and freshwater. *Ecol Lett* 25:1376–1386. doi:10.1111/ele.13999

309 Rosenberg DM, Resh VH, King RS (2008): Use of aquatic insects in biomonitoring. In: Merritt RW,
310 Cummins KW , Berg MB (Editors), *An Introduction to the Aquatic Insects of North America*. Kendall
311 Hunt, Dubuque, IA, pp. 123–138

312 Russakovsky O, Deng J, Su H, Krause J, Satheesh S, Ma S, Huang Z, Karpathy A, Khosla A, Bernstein
313 M, Berg AC, Fei-Fei L (2015) ImageNet Large Scale Visual Recognition Challenge. *Int J Comput Vis*
314 115:211–252. doi:10.1007/s11263-015-0816-y

315 Tickner D et al. (2020) Bending the Curve of Global Freshwater Biodiversity Loss: An Emergency
316 Recovery Plan. *Bioscience* 70:330–342. doi:10.1093/biosci/biaa002

317 Torii T, Abe E, Tare H, Tsuzuki T, Myosho T, Kobayashi T (2023) Prediction of average score per taxon
318 in Japan using mega data from the national census on river environments. *Limnology* 10.1007/s10201-
319 023-00729-2

320 Wightman R (2019): *PyTorch Image Models*. GitHub, GitHub repository

321 Wright IA, Ryan MM (2016) Impact of mining and industrial pollution on stream macroinvertebrates:
322 importance of taxonomic resolution, water geochemistry and EPT indices for impact detection.
323 *Hydrobiologia* 772:103–115. doi:10.1007/s10750-016-2644-7

324 Wright JF (2000): An introduction to RIVPACS. In: Wright JF, Sutcliffe DW, Furse MT (Editors),

325 Assessing the Biological Quality of Fresh Waters: RIVPACS and Other Techniques. Freshwater

326 Biological Association, Ableside, UK, pp. 1–24

327

328

329 Table 1. Number of images in each class in the T- and M-datasets.

Class	T-dataset	M-dataset	Total (train/val)
A: Baetidae	56	219	275 (219/56)
B: Ephemerellidae	130	182	312 (249/63)
C: Heptageniidae	137	212	349 (278/71)
D: Other mayflies	100	74	174 (139/35)

330 Classes were assigned in this study. The images were randomly divided in an 80 (for training, train) to

331 20 (for validation, val) split for each class in each dataset.

332

333 Table 2. Number of images for the test dataset.

Class	Gallery 1	Gallery 2	Total
A: Baetidae	12	6	18
B: Ephemerellidae	12	19	31
C: Heptageniidae	19	20	39
D: Other mayflies	15	17	29

334 The images were collected from two online photo galleries (Gallery 1:

335 <http://museinfo.hitohaku.jp/kawamushi/zukan/kagerou.html>; Gallery 2:

336 <https://www.eonet.ne.jp/~suisseikontyu/>).

337

338

339 **Figure captions**

340 Fig. 1. Example images from the (a) T-dataset and (b) M-dataset.

341

342 Fig. 2. Schematic illustration of the steps to construct a mayfly classification model.

343

344 Fig. 3. (a) Loss function learning curves for training (red) and validation (blue) datasets. (b) Confusion
345 matrix of the 4-class classification in the validation dataset. The numbers denote the number of images
346 belonging to the predicted class, and blue indicates a correct classification. (c) Summary of inferences
347 for the validation dataset. Colored regions indicate the true labels for each image: class A (ID 1–56),
348 class B (ID 57–119), class C (ID 120–190), and class D (ID 191–225). The point data are the predicted
349 labels, as defined in the legend.

350

351 Fig. 4. Example images from classes A–C in the validation dataset. ID numbers are in white; underline
352 indicates misclassification. The incorrectly predicted class and confidence score are shown below each
353 misclassified image.

354

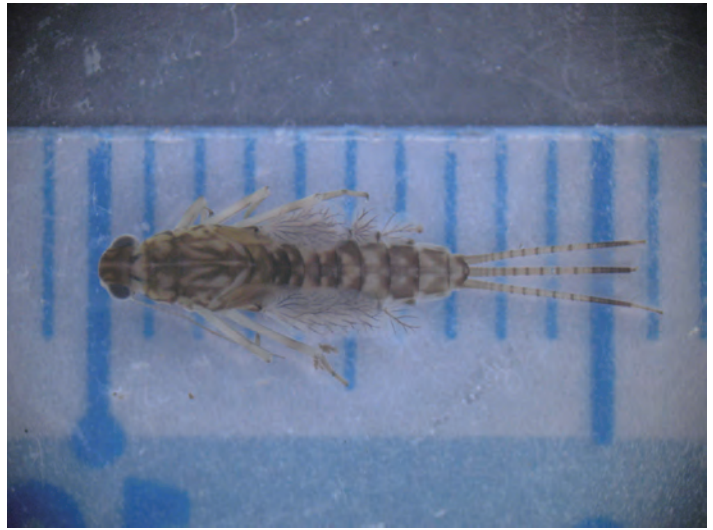
355 Fig. 5. Confusion matrix for the classification task in the test dataset. Top-1 accuracy was 82.9%.

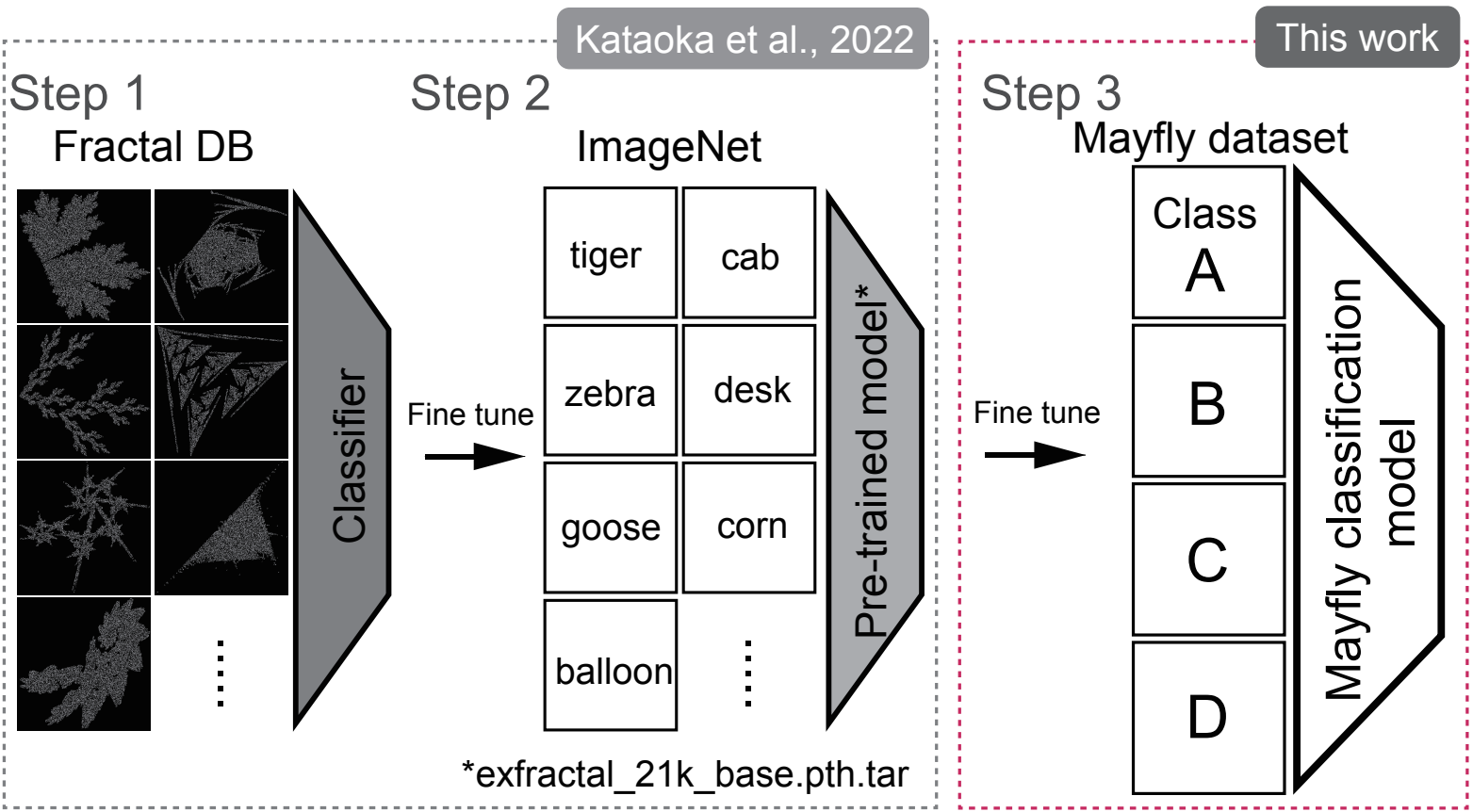
356

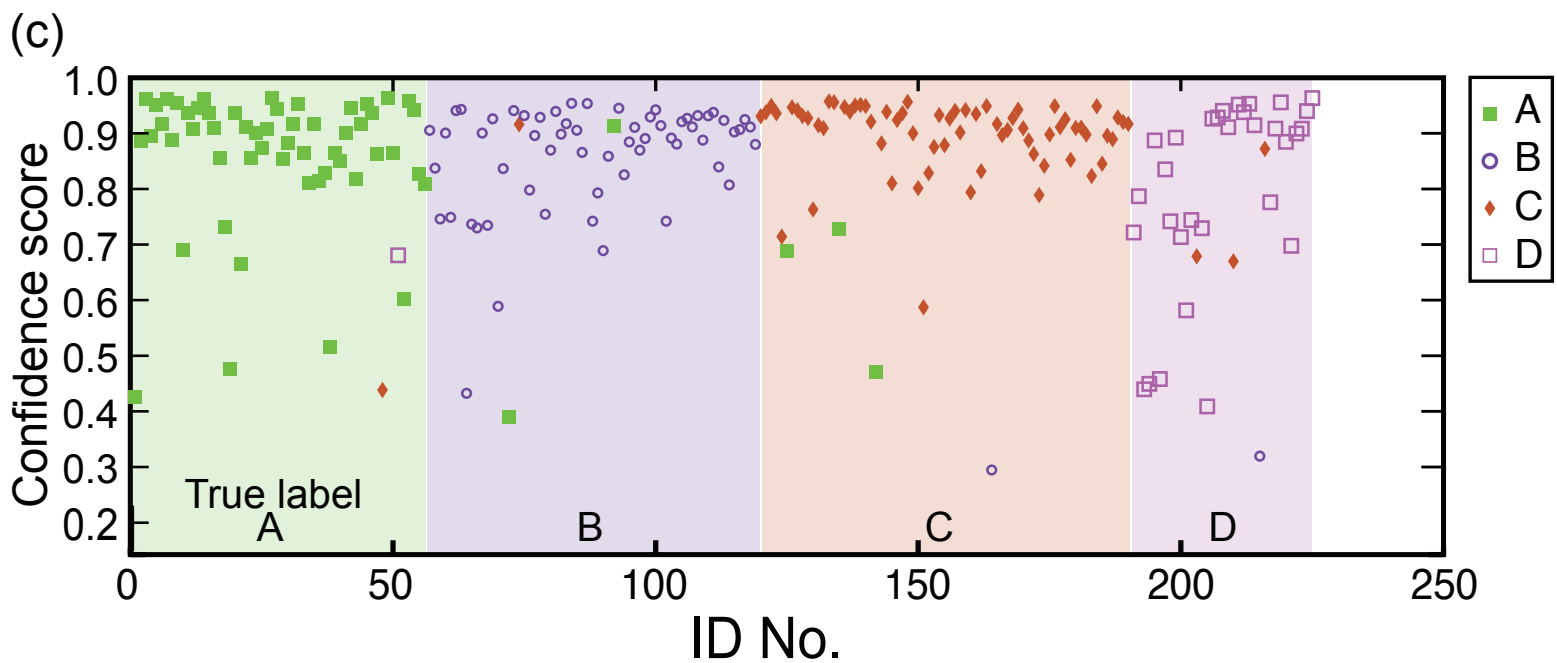
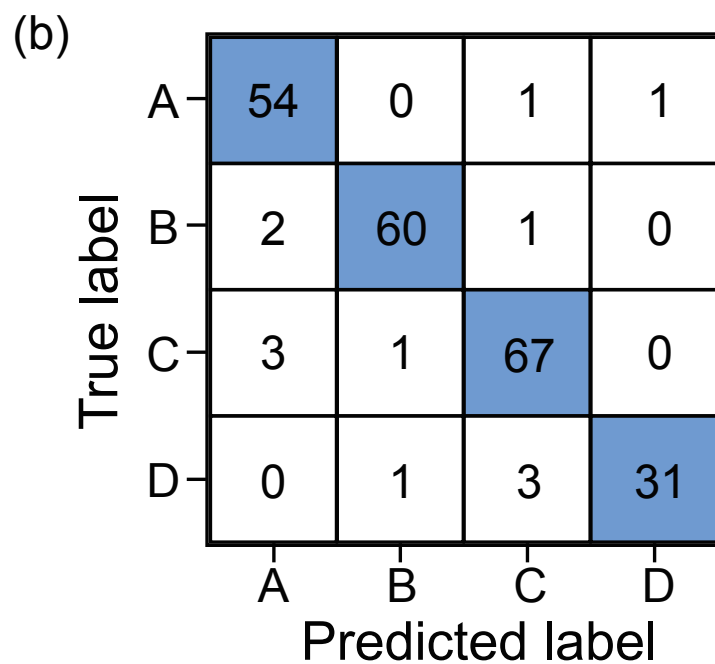
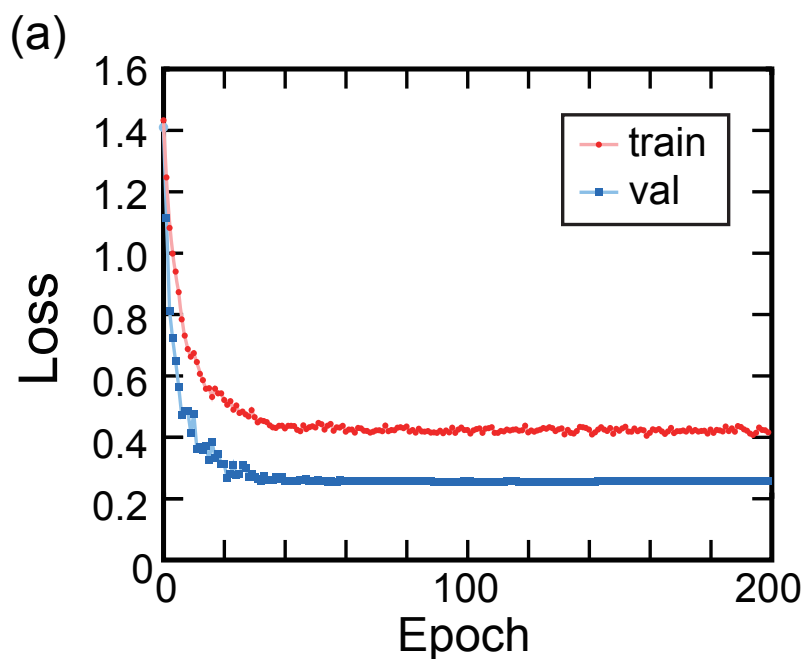
(a)



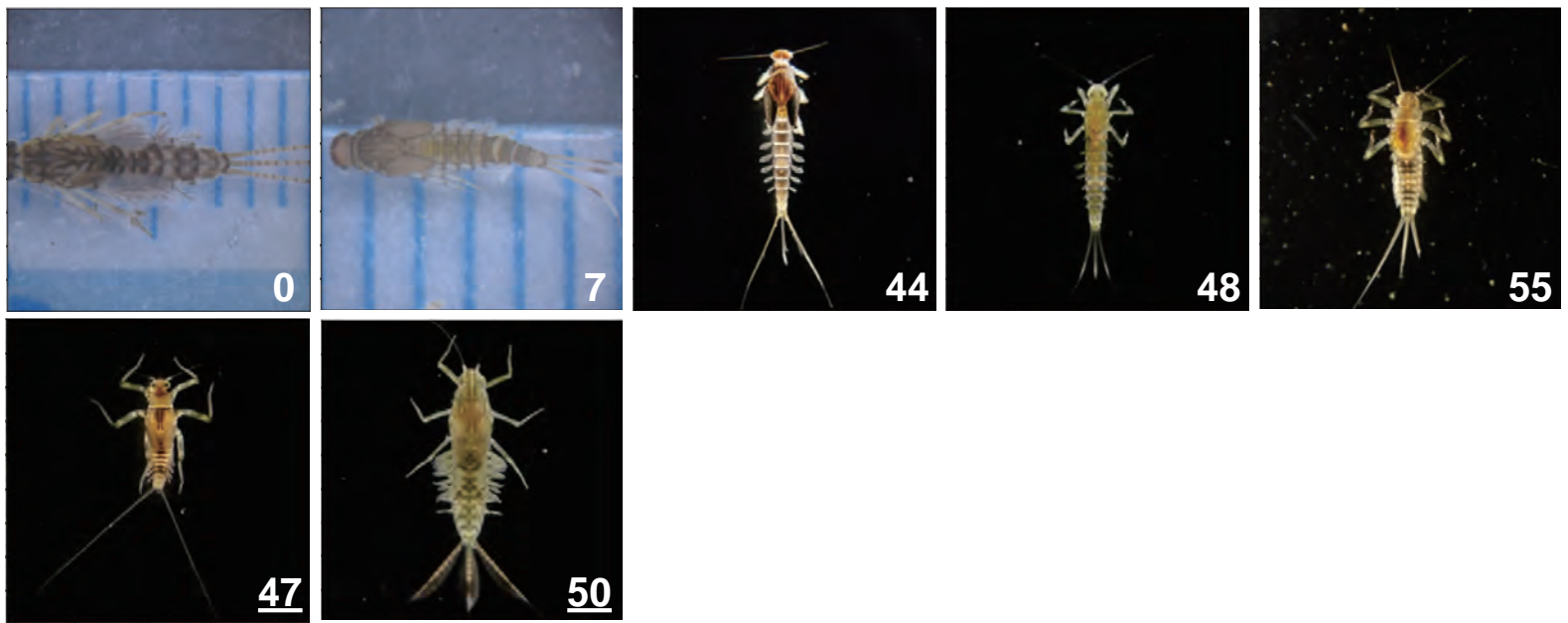
(b)







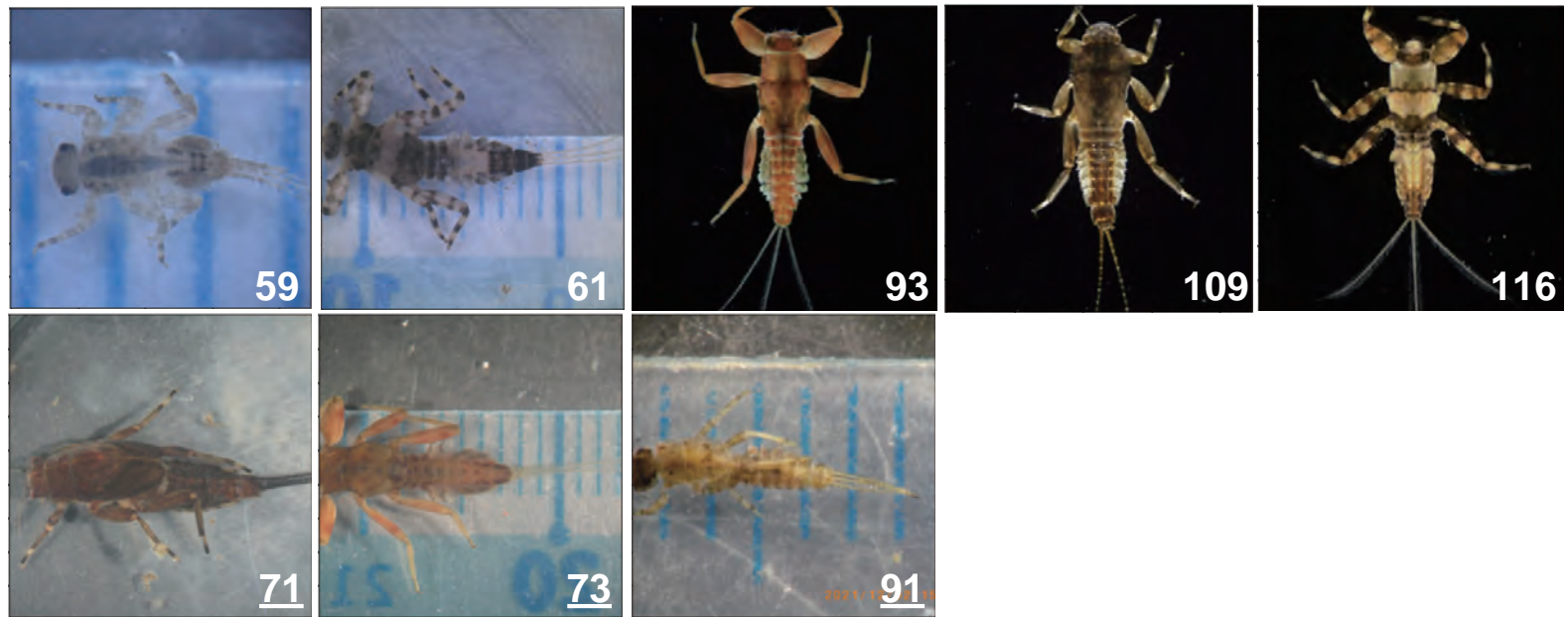
(a) Class A



prediction C: 0.4385

D: 0.6806

(b) Class B

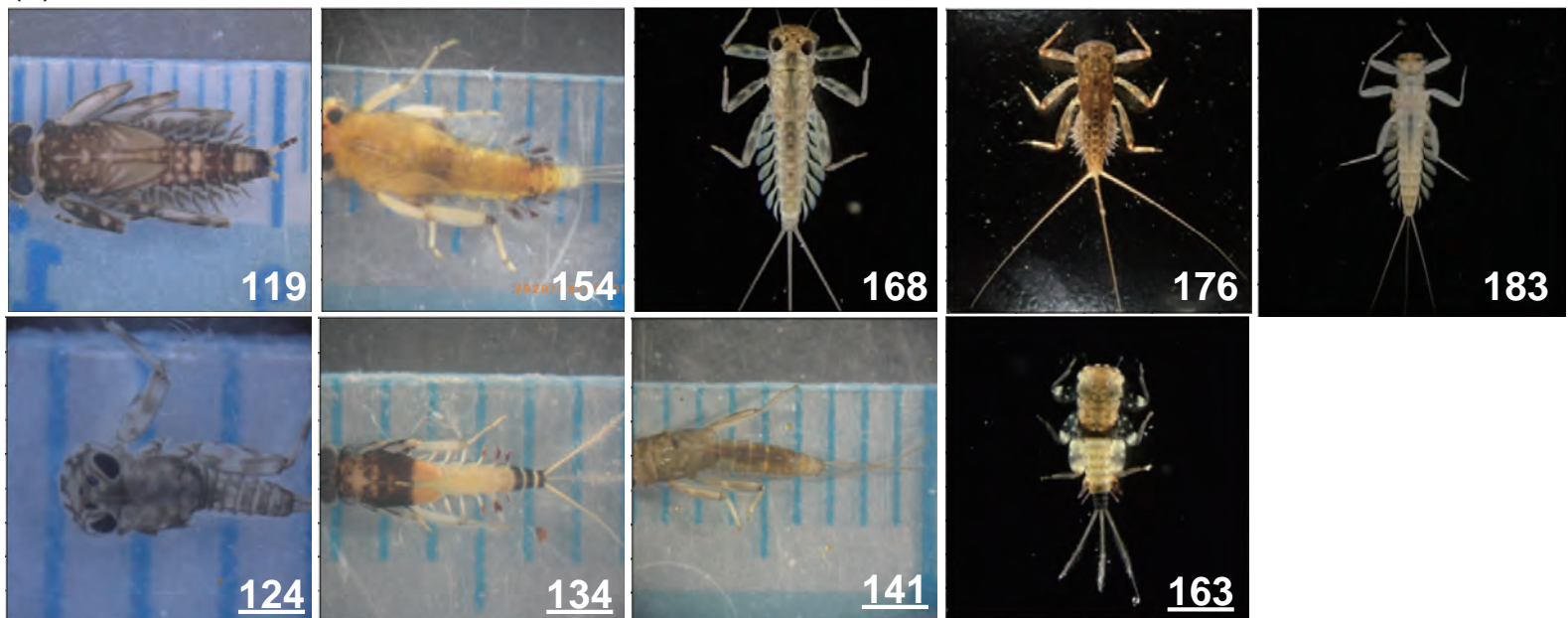


A: 0.3897

C: 0.9161

A: 0.9129

(c) Class C



A: 0.6888

A: 0.7274

A: 0.4710

B: 0.2945

True label

A	17	0	0	1
B	1	25	5	0
C	2	0	37	0
D	2	2	7	18

Predicted label

A B C D

The image displays a confusion matrix for a classification task with four classes: A, B, C, and D. The vertical axis represents the 'True label' and the horizontal axis represents the 'Predicted label'. The matrix is a 4x4 grid where each cell contains the count of instances. The diagonal cells, representing correct classifications, are highlighted in blue. The counts are: True A predicted A: 17; True B predicted B: 25; True C predicted C: 37; True D predicted D: 18. Other counts include True A predicted B: 0, True A predicted C: 0, True A predicted D: 1; True B predicted A: 1, True B predicted C: 5, True B predicted D: 0; True C predicted A: 2, True C predicted B: 0, True C predicted D: 0; True D predicted A: 2, True D predicted B: 2, True D predicted C: 7.